Dynamics of repulsive dual-frequency atomic force microscopy

Robert W. Stark[a)]
Department of Earth and Environmental Sciences and Center for NanoScience (CeNS), Ludwig-Maximilians-Universität München, Theresienstr.41, Munich 80333, Germany

(Received 1 October 2008; accepted 21 January 2009; published online 10 February 2009)

In bimodal atomic force microscopy, two flexural modes are driven at their resonances. The oscillation of the second eigenmode, which is usually an incommensurate multiple of the fundamental frequency, perturbs the dynamic system. Numerical simulations show that the tip motion is almost periodic at typical set points and that harmonics and intermodulation frequencies prevail in the spectrum. The simulations also predict a very small increase in the noise of the first mode amplitude and phase due to the second mode oscillation. At small average tip sample separations, however, phases with repulsive and purely attractive forces can occur intermittently. © *2009 American Institute of Physics*. [DOI: 10.1063/1.3080209]

In a bimodal atomic force microscope (AFM), two flexural modes are simultaneously excited.[1–3] The amplitude of the fundamental mode oscillation is used for topography feedback, while amplitude and phase of the higher mode vibration encode the material composition. The excitation of an additional mode enhances the material specific sensitivity of dynamic AFM.[2–6] Such an enhancement occurs in the attractive[1,6] and in the repulsive regime.[2,4] The excitation at a noninteger or even nonrational multiple ω_2 of the fundamental frequency ω_1, however, introduces a perturbation to the dynamic system because the external driving force $F_d = F_1 \sin(\omega_1) + F_2 \sin(\omega_2)$ is not periodic—or at least the period is very long. In the attractive regime, this perturbation is very small and high contrast and resolution can be achieved at low noise.[3,6] In the repulsive regime, the situation may be different.

In conventional single frequency amplitude modulation, AFM gentle imaging conditions are associated with a stable periodic oscillation state.[7,8] Irregular (chaotic) oscillations can lead to large repulsive tip sample forces.[9] Thus, in order to achieve high resolution and high contrast bimodal AFM in the repulsive regime, the AFM operator needs a guide for the selection of operation parameters (amplitude ratio and set point).

Numerical simulations are a convenient way to investigate the influence of operation parameters on the system dynamics because the repulsive tip-sample forces in bimodal AFM are not accessible experimentally and analytic approximations are not yet available. Here, the cantilever was modeled as a linear and time invariant system. The multiple degree of freedom system was simulated by integrating the state-space equations

$$\dot{\mathbf{x}} = \mathbf{A}\mathbf{x} + \mathbf{b}u,$$

$$\mathbf{y} = \mathbf{C}\mathbf{x}. \tag{1}$$

Matrix **A** describes the cantilever dynamics (resonant frequencies and damping), vector **b** the coupling of the forces u to the individual modes. Matrix **C** accounts for the coupling of the system states **x** to the output **y** (tip position, deflection angle, and velocity).[9,10]

The tip sample interaction was modeled as a nonlinear feedback. The force law was a Derjaguin-Muller-Toporov model with

$$F_{ts}(z) = \begin{cases} -HR/[6(z_s+z)^2] & D \geq a_0, \\ -HR/6a_0^2 + \frac{4}{3}E^*\sqrt{R}(a_0 - z_s - z)^{3/2} & D < a_0, \end{cases} \tag{2}$$

where H is the Hamaker constant, R is the radius of the tip, parameter E^* is the effective contact stiffness, and a_0 is an interatomic distance.

The simulation was implemented with MATLAB 2008a and SIMULINK 7.1 on a Windows PC (Intel Core 2 Duo). The cantilever model was truncated after three eigenmodes. Cantilever parameters were as follows: resonant frequencies $\omega_1 = 1.0$, $\omega_2 = 6.2669$, $\omega_3 = 17.5475$; quality factors $Q_1 = 200$,

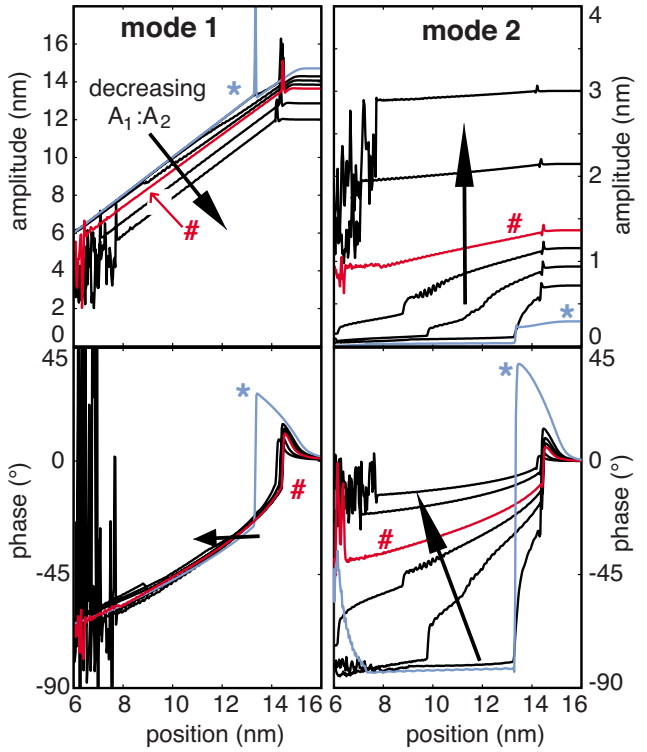

FIG. 1. (Color online) Amplitude and phase curves of both modes for the amplitude ratios $A_1:A_2 = 50$, 20, 15, 12, 10, 6, and 4. The curves with $A_1:A_2 = 50$ (blue) and $A_1:A_2 = 10$ (red) are marked by * and #, respectively. The black arrow indicates the direction of decreasing $A_1:A_2$.

a)Electronic mail: stark@lmu.de. Tel./FAX: +49 89 2180-4329/-4334.

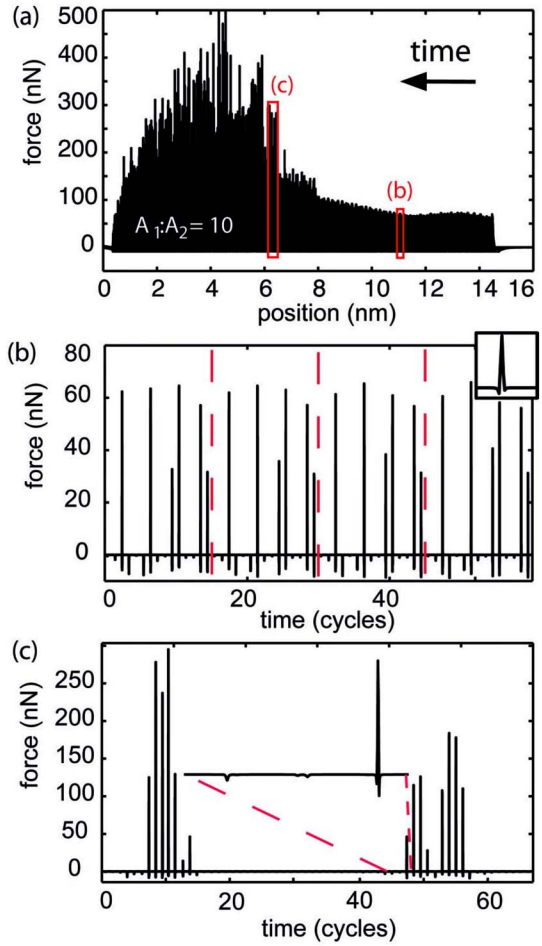

FIG. 2. (Color online) (a) Interaction forces during approach for $A_1+A_2=15$ nm (red curve # in Fig. 1). The frames for both time series are indicated. (b) Time series data in a quasiperiodic regime. A period of 15 oscillations prevails for $\hat{A}_1/A_1=80\%$. (c) Time series obtained in the intermittent regime. Phases of noncontact and repulsive contact occur intermittently. The insets in (b) and (c) show typical force pulses.

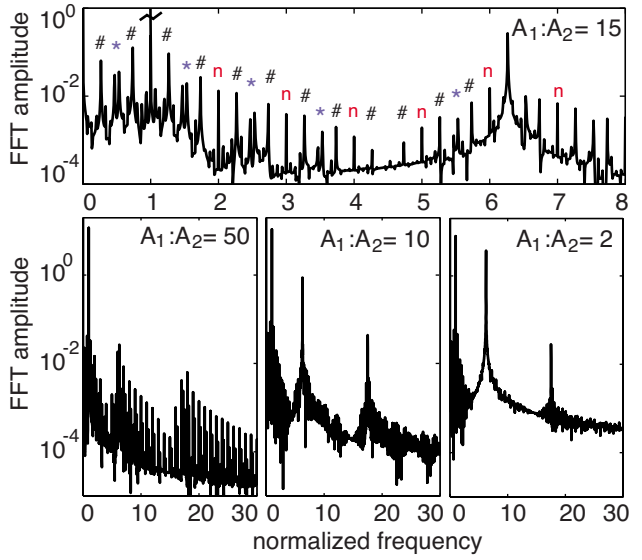

FIG. 3. (Color online) FFT spectra at $\hat{A}_1/A_1=80\%$ for various amplitude ratios. For $A_1:A_2=15$ the harmonics of the driving frequency (n) and intermodulation products are indicated. Frequencies following the rule $\omega=\pm\omega_2\pm n\omega_1$ are marked by "#" and those according to $\omega=\pm 2\omega_2\pm n\omega_1$ by "*."

$Q_2=400$, $Q_3=400$, tip radius $R=20$ nm, spring constant $k=10$ N/m. Material parameters were $E^*=156$ GPa and $a_0=0.16$ nm. The system was integrated with the variable step solvers ode15s and ode45 in MATLAB/SIMULINK in the "rapid acceleration" mode. Both solvers yielded similar results. The maximum integration step width was set to $t=2\pi/1280$. "Zero crossing" detection was enabled to precisely calculate the transition at a_0 in Eq. (2).

The simulations focused on the parameter range used for imaging in bimodal AFM.[2,4,6,11] The excitation frequencies were set to $\omega_{dr}^{(1)}=\omega_1$, $\omega_{dr}^{(2)}=\omega_2$. In order to compare simulations for different amplitude ratios, the composite free amplitude was set to $A_0=A_1+A_2=15$ nm. The second mode amplitude was kept smaller than the first one ($A_1>A_2$). In the following, the hat denotes values under tip sample interaction. Thus, $\hat{A}_i$ is the average oscillation amplitude with tip sample interaction and A_i the free amplitude without. Amplitudes and phases were calculated by a sliding fast Fourier transform (FFT) with a rectangular window (128 cycles at ω_1 width and 50% overlap).

Figure 1 shows approach curves for different amplitude ratios $A_1:A_2$. The shape of the amplitude curve (first mode) was only weakly affected by the second mode excitation. The slope of the amplitude response of the second eigenmode, however, varied during approach. Without second mode excitation, the system remained in the noncontact regime, also referred to as attractive regime or low amplitude solution (data not shown).[7,8] For $A_1:A_2>50:1$ (blue, * in Fig. 1) the response changed at 13.4 nm. The system transited from a regime with purely attractive to a regime with repulsive interaction forces. The transition was induced by the perturbation caused by the higher mode excitation. This result confirms the experimental observation of a stabilized repulsive regime in bimodal AFM.[12]

The amplitude of the second mode dropped significantly during the transition and the second mode phase became insensitive to the approach. For decreasing ratios the amplitude $\hat{A}_2$ was less affected. The amplitude and phase curves for $A_1:A_2=10$ (red, # in Fig. 1) responded continuously to the variation in the tip sample contact. At separations smaller than $z=6$ nm the amplitude and phase curves became very noisy.

The general shape of the amplitude and phase response can be understood by comparing the energy stored in both modes. For large amplitude ratios (e.g., $A_1:A_2=50:1$), the energy ratio is $E_1/E_2=\omega_1^2A_1^2/\omega_2^2A_2^2\gg 1$. Much more energy is stored in the first than in the second mode. Thus, the response of the first mode dominates. For ratios $E_1/E_2<1$ (e.g., $A_1:A_2=4:1$), however, the second mode contains most of the energy. At intermediate amplitude ratio of $A_1:A_2\approx 10:1$, the energy stored in both modes is of the same order of magnitude leading to a similar phase response at both modes.

Figure 2(a) displays the interaction forces during approach for $A_1:A_2=10$. The peak forces were in the order of 100 nN in the regime dominated by the first mode. At a position of $z<7$ nm and less, the repulsive peak forces increased to a maximum of 500 nN. At $z=7$ nm, the amplitudes also dropped to $\hat{A}_1=6.4$ nm and $\hat{A}_2=0.95$ nm. At this point, the energy stored in both modes was comparable, since $\hat{E}_1/\hat{E}_2=\omega_1^2\hat{A}_1^2/\omega_2^2\hat{A}_2^2\approx 1$. Figure 2(b) shows indi-

TABLE I. Mean values and standard deviation (brackets) of amplitude and phase values. Last line: $A_1=15$ nm, $A_2=7.5$ nm.

$A_1:A_2$	$\langle\hat{A}_1\rangle$ (nm)	$\langle\hat{A}_2\rangle$ (nm)	$\langle\phi_1\rangle$ (deg)	$\langle\phi_2\rangle$ (deg)
$A_1=15$ nm	12.0(9.1e−8)	⋯	+36.2(9e−12)	⋯
50:1	11.8(2.2e−5)	0.05(7.2e−6)	−36.7(0.001)	−83.6(0.013)
10:1	10.9(2.4e−4)	1.8(2.2e−4)	−35.6(0.006)	−19.27(0.009)
5:1	10.0(4.8e−4)	3.4(5.1e−4)	−35.8(0.009)	−9.24(0.007)
2:1	8.0(9.7e−4)	7.0(8.0e−4)	−36.0(0.016)	−3.7(0.005)
2:1[a]	12.0(9.7e−4)	6.9(4.0e−4)	−36.1(0.010)	−5.4(0.005)

[a]Total amplitude $A_1+A_2=15$.

vidual force pulses at a set-point of 80%. After 15 cycles the force pattern is almost repeated, which indicates a quasiperiodic regime. This means that the oscillation is almost periodic microscopically, but may be not periodic macroscopically. Within a period, the maximum peak force was highly variable.

At smaller positions z, the second mode dominates the tip sample interaction since $\hat{E}_2>\hat{E}_1$. No periodic response could be identified and the interaction force followed an irregular pattern [Fig. 2(c)]. Time periods with repulsive as well as purely attractive forces occurred intermittently. The inset shows individual force pulses (repulsive and attractive). The intermittent dynamics encountered here also explains the instable phase signal shown in Fig. 1. Note that the simulations neglect energy dissipation in the tip sample contact, which may play an important role in the stabilization of the quasiperiodic regime.

In Fig. 3, FFT spectra of the tip displacement for an amplitude set-point of $\hat{A}_1/A_1=80\%$ are given for various amplitude ratios. Harmonics and intermodulation products prevail in the spectrum [Fig. 3(a)]. Such intermodulation frequencies occur due to the nonlinear tip sample contact.[13,14] The harmonics of the fundamental frequency $\omega=n\omega_1$ are indicated by the letter n. Since the harmonics were very prominent in the spectrum; also intermodulation products of very high order were present. Figure 3(b) illustrates the effect of increasing second mode excitation. At $A_1:A_2=50$, the spectrum shows well-defined harmonics and intermodulation products. By increasing the amplitude ratio, their peaks broaden. This broadening is due the quasiperiodic oscillation, where the instantaneous partial frequencies are only nearly harmonic frequencies. With the amplitude ratio increasing to $A_1:A_2=2$ the instantaneous frequencies of the harmonics peaks were severely detuned from their periodic values and the distinct harmonic and intermodulation peaks vanished. This effect implies that the trajectory was no longer periodic macroscopically.

Experimentally, the excitation of an additional mode also might imply additional noise. In order to evaluate the noise caused by the second mode, a line scan on a flat surface was simulated for the set-point $\hat{A}_1/A_1=80\%$. A sliding window FFT (window size: 256 cycles, without overlap) was used to calculate amplitudes and phase (Table I). The standard deviation of $\hat{A}_1$ increased by several orders of magnitude (from 9×10^{-8} to 2×10^{-5} nm) due to the second mode excitation ($A_1:A_2=50$). The standard deviation increased further to 1×10^{-3} nm for $A_1:A_2=2$. Such a subpicometer noise, however, will be irrelevant in practical measurements since typical measurement noise is larger. Nevertheless, these amplitude fluctuations (process noise) are responsible for the stabilization of the repulsive regime. The second mode amplitude is less sensitive. At large A_2 ($A_1:A_2=2$, $A_1=15$ nm, $A_2=7.5$ nm) the amplitude noise of the second mode is reduced. At this amplitude ratio ($A_1:A_2=2$, $E_1<E_2$) the first mode responded to the decreasing distance ($\hat{A}_1/A_1=80\%$), while $\hat{A}_2$ only slightly varied ($\hat{A}_2/A_2=92\%$).

In summary, the simulations predict that quasiperiodic and intermittent regimes can exist in bimodal AFM depending on the operating conditions. In the intermittent regime, oscillation cycles with repulsive and purely attractive interaction forces occur intermittently. This type of dynamics is predicted for small amplitude ratios $A_1:A_2$ or small set-points. The simulations also show that in the quasiperiodic regime stable imaging is possible because the additional amplitude noise caused by the second mode excitation is very small. Although amplitude fluctuations are small, the peak forces can vary considerably. The amplitude ratio is a key parameter for the amplitude and phase response. In the case of $A_1\gg A_2$, the dynamics is dominated by the first mode response. For imaging in the noncontact regime, the amplitude ratio thus should be adjusted to $A_1\gg A_2$ in order to obtain sensitive and stable imaging. In the repulsive regime, the sensitivity of the second eigenmode phase can be increased by increasing A_2. The operator will have to balance sensitivity and strength of interaction forces.

Financial support by the DFG excellence cluster "Nanosystems Initiative Munich (NIM)" and the European Commission (Grant No. NMP4-CT-2004-013684) is gratefully acknowledged.

[1]T. R. Rodriguez and R. Garcia, Appl. Phys. Lett. **84**, 449 (2004).
[2]R. Proksch, Appl. Phys. Lett. **89**, 113121 (2006).
[3]N. F. Martinez, S. Patil, J. R. Lozano, and R. Garcia, Appl. Phys. Lett. **89**, 153115 (2006).
[4]C. Dietz, M. Zerson, C. Riesch, A. M. Gigler, R. W. Stark, N. Rehse, and R. Magerle, Appl. Phys. Lett. **92**, 143107 (2008).
[5]J. R. Lozano and R. Garcia, Phys. Rev. Lett. **100**, 076102 (2008).
[6]S. Patil, N. F. Martinez, J. R. Lozano, and R. Garcia, J. Mol. Recognit. **20**, 516 (2007).
[7]R. Garcia and A. San Paulo, Phys. Rev. B **60**, 4961 (1999).
[8]R. Garcia, R. Magerle, and R. Perez, Nature Mater. **6**, 405 (2007).
[9]R. W. Stark, Nanotechnology **15**, 347 (2004).
[10]R. W. Stark, G. Schitter, M. Stark, R. Guckenberger, and A. Stemmer, Phys. Rev. B **69**, 085412 (2004).
[11]R. W. Stark, N. Naujoks, and A. Stemmer, Nanotechnology **18**, 065502 (2007).
[12]P. Thota, S. MacLaren, and H. Dankowicz, Appl. Phys. Lett. **91**, 093108 (2007).
[13]D. Platz, E. A. Tholen, D. Pesen, and D. B. Haviland, Appl. Phys. Lett. **92**, 153106 (2008).
[14]M. T. Cuberes, H. E. Assender, G. A. D. Briggs, and O. V. Kolosov, J. Phys. D **33**, 2347 (2000).